Growth and characterization of Cu-catalyzed ZnO nanowires

2007 J. Phys.: Conf. Ser. 61 703

(http://iopscience.iop.org/1742-6596/61/1/141)

IOP Publishing Journal of Physics: Conference Series **61** (2007) 703–707
doi:10.1088/1742-6596/61/1/141 International Conference on Nanoscience and Technology (ICN&T 2006)

Growth and characterization of Cu-catalyzed ZnO nanowires

Y M Zhao,[1] Y H Li,[1] Y Z Jin,[2] X P Zhang,[2] W B Hu,[1] I Ahmad,[1] G McCartney,[1] Y Q Zhu[1]*

1 School of Mechanical, Materials and Manufacturing Engineering,University of Nottingham, University park, Nottingham NG7 2RD UK
2 Cavendish Laboratory, University of Cambridge, Madingley Road, Cambridge CB3 0HE, UK

Email: yanqiu.zhu@nottingham.ac.uk

Abstract. Cu-catalyzed ZnO nanowires have been synthesized by thermal evaporation of Cu-Zn powder alloys in a water vapor atmosphere. The diameters of the nanowires can be controlled by the amount of water vapor introduced into in the reaction tube. Raman spectroscopic characterization reveals two additional modes at 621 and 671cm^{-1} which are indicative of the existence of host-lattice defects caused by Cu doping or other intrinsic lattice defects that formed during the nanowire growth. Field emission and photoluminescence (PL) properties of Cu-catalyzed ZnO nanowires have also been investigated using nanowires with a diameter of 20 nm and 200 nm. The field emission results show that the thinner nanowires have a lower turn-on electrical field than the thicker ones, whilst both nanowires exhibit a similar field emission enhancement factor in the high electric field region. In the PL spectra, we have observed a blue-shift of the UV emission peak and a red-shift of the green emission peak when the nanowire diameters decreased from 200 nm to 20 nm.

1. Introduction

As an interesting wide bandgap (3.3ev) semiconductor material, ZnO has numerous promising applications in electronic and optical devices [1-4]. Due to the intrinsic defects such as oxygen vacancies and zinc interstitials, one dimensional ZnO nanowires usually behave as n-type semiconductors. The major impediment for actual application of ZnO nanowires in electronics and photonics lies in the difficulties of achieving p-type doping [5-6]. It is noted that the electrical and optical properties of the semiconductors can be tuned by various doping processes for special applications. Except for doping, the properties of these semiconducting nanowires are affected by their preparation techniques. Cu-doped ZnO has attracted considerable attention in bulk and thin film forms because it is theoretically believed that doping with Cu may realize a p-type ZnO [7-9]. In fact, it has been reported that ZnO nanowires exhibit different band gaps when catalyzed by Au and Cu during their formation, which is due to the impurities incorporated into their structures [10]. Recently, Cu-doped ZnO nanowires have been synthesized by a hydrothermal method using CuI and ZnI_2 and the photoluminescence profiles of the nanowires show significant red-shifts due to the changes of the electron energy levels in the forbidden band [11]. In order to obtain such Cu-catalyzed ZnO nanowires, most processes have involved the sputtering of a thin Cu film on a Si substrate on which the ZnO nanowires grow [12-13]. In this context, we demonstrate the generation of ZnO nanowires by a simple thermal evaporation of Cu-Zn powder alloys in a water vapor atmosphere at 1000-1100°C.

The electron field emission and photoluminescence emission properties (PL) of the resulting nanowires are also reported.

2. Experimental

The experimental set-up consists of a horizontal tube furnace with a ceramic working tube of ϕ50 × 500 mm, a quartz reaction tube of ϕ35× 1000 mm, and a mass gas flow control system. A Cu-Zn alloy powder (70/30 atm%, 60 mesh, Aldrich) was treated using acetone, then dispersed uniformly on a quartz plate (20 ×20 mm), and the plate was then loaded to the middle of the reaction tube. High purity argon (>99.995%) was bubbled through deionized water contained in a wash-bottle and then passed through the hot reaction tube, with adjustable flow rates in order to achieve different amounts of water vapor in the reaction tube. Prior to heating, the reaction tube was thoroughly flushed for 30 min with argon to eliminate air residue in the system. A Si substrate was placed at the downstream position of the reaction tube about 10-15 cm away from the Cu-Zn precursor.

After heating for 1 hr at 1000-1100°C, the deposit on the Si substrate where the temperature was measured between 400-450°C was collected. The as-prepared sample was examined by scanning electron microscopy (SEM Philips XL30), X-Ray diffractometer (XRD, Siemens D500), transmission electron microscopy (TEM, JEOL 2000FX operated at 200 kV) and high resolution TEM (JEM-3000F JEOL operated at 300 kV). The field emission property was measured in a chamber under a vacuum of less than 2×10^{-6} Torr, using a parallel diode structure with an anode-cathode spacing of 250 μm, and an indium-tin-oxide coated glass plate as the anode. The PL emission spectrum was recorded by a Cary Eclipse Fluorescence Spectrophotometer, using a 325 nm Hd-Cd laser as the excitation light source.

3. Results and discussion

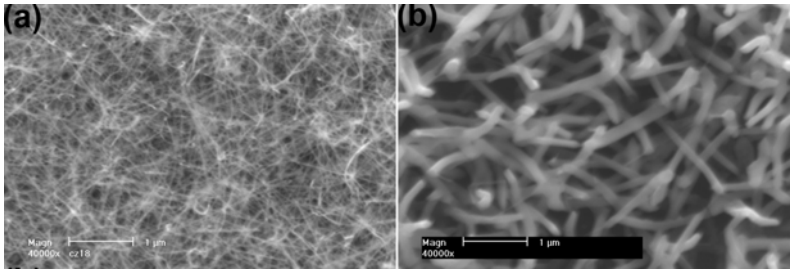

Figure 1 SEM images of Cu-catalyzed ZnO nanowires grown at 1000 °C for 1h.
(a) using an Ar flow rate of 30 sccm, (b) using an Ar flow rate of 200 sccm.

Figure 1 shows the SEM images of the resulting Cu-catalyzed ZnO nanowires after 1 h growth at 1000°C. As we have fixed all other parameters during the heating process, it is apparent that the diameters of the ZnO nanowires are dependent on the Ar flow rates which actually determine the amount of water vapor in the reaction tube. Low flow rate (< 100 sccm) results in fine nanowires with a uniform diameter of ca. 20 nm (Figure 1a) and high flow rate (> 200 sccm) leads to coarse nanowires of ca. 200 nm in diameter (Figure 1b). The vapor is likely to decompose when passed over the hot zinc surface, following the reaction ($Zn + H_2O \rightarrow ZnO + H_2$). When the temperature is higher than the melting point of the Cu-Zn (30%) alloy, Cu will work as a catalyst to promote the growth of ZnO nanowires, via thermal evaporation and condensation process.

The composition and the microstructure of the obtained nanowires were investigated by XRD and TEM. The XRD pattern of the Cu-catalyzed ZnO nanowires (diameters around 20 nm) is shown in Figure 2. The peaks are indexed to the hexagonal wurtzite ZnO structure and there is no trace of Cu or CuO peaks. In the XPS spectrum (data not shown) also indicated there are no contaminant species. Figures 3a and 3b display the TEM and HRTEM images of the nanowires. The characteristic of the existence of a nanoparticle at the nanowire tip that usually acts as catalyst, e.g. the dark particles shown in Figure 3a, is indicative of a possible vapor-liquid-solid (VLS) growth mechanism for the

ZnO nanowires [3,14]. The lattice fringes in Figure 3b give a *d*-spacing of ca. 0.52 nm, corresponding to the (001) plane perpendicular to the grow direction. The corresponding electron diffraction (ED) pattern (inset) confirms the single-crystal nature of the nanowires.

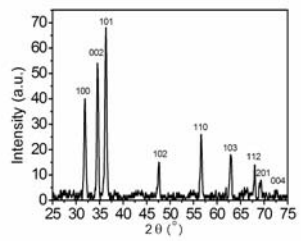

Figure 2 XRD pattern of the resulting ZnO nanowires

The Raman spectrum of the nanowires with diameters of around 20 nm was recorded, as shown in Figure 4. Bulk ZnO is expected to have peaks at 101 cm^{-1} (E2), 380 cm^{-1} (A1, TO), 407 cm^{-1} (E1, TO), 437 cm^{-1} (E2), and 583 cm^{-1} (E1, LO) [15]. Comparing these so-called classical peaks with the present results, we find only the E2 band at 437 cm^{-1}, all other peaks being absent. The appearance of a strong

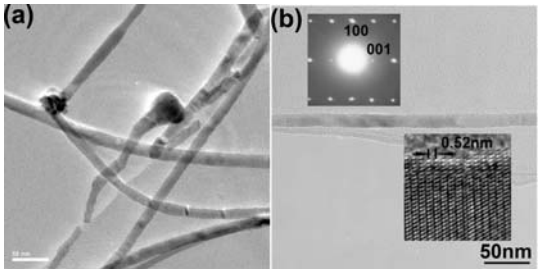

Figure 3 (a) and (b) TEM (inset are ED pattern and HRTEM) images of the ZnO nanowires.

peak at 302 cm^{-1} could be due to the activation of the B2 silent mode, which reportedly exists between 250 and 300 cm^{-1} in phonon dispersion curves of single crystalline ZnO [16]. The shoulder to 225 cm^{-1} could be attributed to the oxygen vacancies, and a similar appearance of the mode at 221 cm^{-1} has previously been reported in ZnO thin films. Both of the B2 silent mode and the oxygen vacancy mode are red-shifted compared with the previous results. It is noteworthy that there are two additional weak bands at 621 and 671 cm^{-1}. Modes at 664 and 660 cm^{-1} have also been found in pure ZnO nanostructures which were attributed to the multi-phonon processes or to the intrinsic host-lattice defects [17-18]. Recently, doped ZnO nanopowders or nanowires have been reported, such as $Zn_{1-x}Mn_xO$ and $Zn_{1-x}Mn_xO$ [19-20], and the two vibration mode at 600 and 670 cm^{-1} are always detected in these doped nanostructures. Lattice or intrinsic host-lattice defects are activated when an alien ion

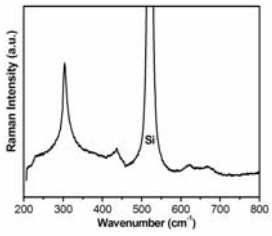

Figure 4 Raman spectrum of the resulting ZnO nanowires

occupies the Zn sites, leading to additional vibration modes. Therefore, the two peaks at 621 and 671 cm^{-1} may suggest the existence of host-lattice defects that might be caused by Cu or other intrinsic lattice defects formed during the nanowire growth. These additional vibration modes are of great importance because they will influence the scattering of propagating electrons within the nanowire structures and modify the optoelectronic performance of the nanowires. Note that however, the two weak peaks may also associated with the Si substrate, as a combination of acoustic and optical

phonons at different symmetric points in the Brillouin zone of the Si lattice could also result in the two-phonon Raman peaks.[21]

Figure 5 shows the field emission current versus applied voltage plots of the nanowires. The shape, size, diameter and distribution of the two nanowire samples are shown in Figure 1. The turn-on electrical fields under the current density of 10 $\mu A/cm^2$ are 3.2 and 4.1 V/μm for the nanowires with diameter of 20 and 200 nm, respectively. The thin nanowires exhibit a lower turn-on field, owing to their sharper tips and higher aspect ratio. The field emission property was also evaluated according to the Fowler-Nordheim (F-N) theory [22], as shown in Figure 5. In the F-N model, the electron emission from a semi-infinite flat metallic surface can be expressed in terms of current density (J) and electric field (E) as: $J = A (\beta^2E^2/\phi)\exp(-B \varphi^{3/2} / \beta E)$, where A and B are constants with A=1.54 × 10-10 (AV^{-2} eV) and B=6.83× 109 (V m^{-1} $eV^{-3/2}$) and ϕ is the work function. β is the field enhancement factor of the sample, determined by tracing the F-N plot through ln(J/E2) versus 1/E following a linear

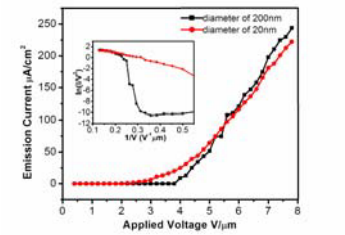

Figure 5 Field emission profiles of the ZnO nanowires and the F-N plots

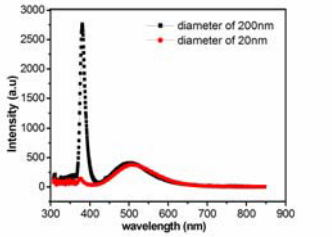

Figure 6 PL spectra of the ZnO nanowires

relationship. From Figure 5, it is apparent that the F-N plot of the thin nanowires (20 nm diameter) displays a straight line. By adopting the work function of ZnO (5.37 eV) [23], β is determined to be 8900. This value is high enough for nanowires applications in field emission display devices. The thicker nanowires (200 nm diameter) only exhibit a linear F-N plot when the applied electric field is larger than 5 V/μm, and these points in the low electric field region (< 3 V/μm) indicate no electron emission from the sample. When the applied electron field is larger than 5 V/μm, the F-N plot of the thick nanowires displays the same slope to that of the thin nanowires, indicating an equivalent field enhancement factor, β. It is generally assumed that β is related to the nanowire shape, size and nanowire density. The results in Figure 5 demonstrate the diameter effect and show that the thinner sample has a lower turn-on electric field, whilst the thicker nanowires has the same field enhancement factor β to the thinner ones in the high electric field region.

Figure 6 displays the PL spectra of the ZnO nanowires of 20 nm and 200 nm in diameter. Typical ZnO bulk crystals have reportedly showed a UV emission (at about 380 nm), due to the near band edge emission of the wide band gap ZnO, and broad green emissions at 510 to 550 nm owing to the deep-level or trap-state emission [24-25]. It seems that the ZnO nanowires with a diameter of 200 nm exhibit a sharp and strong UV emission peak at 380 nm and a broad green emission peak at ca. 500 nm. However, for the thinner (20 nm in diameter) nanowires, the UV emission peak decreases significantly and a 6 nm blue-shift to 374 nm has been observed; the green emission peak shows similar intensity with a red-shift of 6 nm to 506 nm. A blue shift of 14 nm for the UV emission peak has been reported using ZnO nanowires of 6 nm and 200 nm in diameter [26].Yang et. al. have reported the PL spectra of Au-catalyzed ZnO nanowires with different diameters [24], and found no shift for the UV emission peak at 380 nm for all the samples, and all these peaks remain sharp and strong. The intensity of the green emission at around 520 nm has increased as the nanowire size decreases and a slight blue-shift has been recognized. As shown in Figure 6, the shift of the UV emission peak suggests the change of the optical band gaps of the sample, and the shift of the green emission peak indicates the change of the defect levels in the nanowires. The incorporation of Cu impurities during the growth will contribute to the modification of the band gaps and the defective levels. Thinner nanowires have a higher surface area to volume ratio, which might favor a higher level

of surface and deep-level oxygen vacancy or other surface and deep-level defect sites. Therefore, the ratio of the green emission increases as the diameter of the nanowires decreases.

4. Conclusion

In conclusion, we have successfully synthesized Cu-catalyzed ZnO nanowires using a thermal evaporation of Cu-Zn powder alloys in a water vapor atmosphere at 1000-1100°C. The diameters of the nanowires can be controlled by the amount of water vapor introduced into in the reaction tube. XRD and TEM investigations show that the ZnO nanowires are single crystalline growing along the <001> axis of the hexagonal wurtzite ZnO structure. The two additional modes at 621 and 671 cm^{-1} may indicate the probable existence of host-lattice defects which may be caused by the Cu doping or other intrinsic lattice defects formed during the nanowire growth. Field emission and PL measurements have been conducted using nanowires with two diameters of 20 nm and 200 nm. The field emission results show that thinner nanowires have a lower turn-on electric field than the thicker nanowires. Nanowires with different diameters display a similar field emission enhancement factor in the high electric field region. The PL studies reveal a blue-shift of the UV emission peak and a red-shift of the green emission peak when the diameters of the nanowires decrease from 200 nm to 20 nm.

References

[1] Wang Z L, 2003 *Nanowires and Nanobelts – Materials, Properties and Devices, Nanowires and Nanobelts of Functional Materials,* vol. II (Kluwer Academic Publisher, Dordrecht)
[2] Comini E, Faglia G, Sberveglieri G, Pan Z W, Wang Z L, 2002 *Appl. Phys. Lett.* **81** 1869
[3] Huang M H, Mao S, Feick H, Yan H Q, Wu Y Y, Kind H, Weber E, Russo R, Yang P D, 2001 *Science* **292** 1897
[4] Wu J J, Liu S C, Wu C T, Chen K H, Chen L C, 2002 *Appl. Phys. Lett.* **81** 1312
[5] Yan Y, Zhang S B, Pantelides S T, 2001 *Phys. Rev. Lett.* **86** 5723
[6] Xiong G, Wilkinson J, Mischuck B, Tuzemen S, Ucer K B, Williams R T, 2002 *Appl. Phys. Lett.* **80** 1195
[7] Dingle R, 1969 *Phys. Rev. Lett.* **23** 579
[8] Lee J B, Lee H J, Seo S H, Park J S, 2001 *Thin Solid Films* **61** 398
[9] Park W I, Jun Y H, Jung S W, Yia G C, 2003 *Appl. Phys. Lett.* **82** 964
[10] Li S Y, P. Lin, Lee C Y, Tseng T Y, 2004 *J. Appl. Phys.* **95** 3711
[11] Zhou S M, Zhang X H, Meng X M, Zou K, Fan K. Wu S K, Lee S T, 2004 *Nanotechnology* **15** 1152
[12] Li S Y, Lee C Y, Tseng T Y, 2003 *J. Cryst. Growth* **247** 357
[13] Xu C X, Sun X W, Zhang X H, Ke L, Chua S J, 2004 *Nanotechnology* **15** 856
[14] Huang M H, Wu Y, Feick H, Weber E, Yang P, 2001 *Adv. Mater.* **13** 113
[15] Mcguire K, Pan Z W, Wang Z L, Milkie D, Menendez J, Rao A M, 2002 *J. Nanosci. Nanotech.* **2** 499
[16] Calleja J M, Cardona M, 1977 *Phys. Rev. B* **16** 3753
[17] Chen S J, Liu Y C, Shao C L, Mu R, Lu Y M, Zhang J Y, Shen D Z, Fan X W, 2005 *Adv. Mater.* **17** 586
[18] Yang L W, Wu X L, Huang G S, Qiu T, Yang Y M, 2004 *J. Appl. Phys.* **97** 014308
[19] Bergman L, Morrison J L, Chen X B, Huso J, Hoeck H, 2006 *Appl. Phys. Lett.* **88** 023103
[20] Cong C J, Liao L, Liu Q Y, Li J C, Zhang K L, 2006 *Nanotechnology* **17** 1520
[21] Kumar B, Gong H, Vicknesh S, Chua S J, Tripathy S, 2006 *Appl. Phys. Lett.* **89** 141901
[22] Gadzuk J W, Plummer E W, 1973 *Rev. Mod. Phys.* **45** 487
[23] Lee C J, Lee T J, Lyu S C, Zhang Y, Ruh H, Lee H J, 2002 *Appl. Phys. Lett.* **81** 3648
[24] Yang P, Yan H, Mao S, Russo R, Johnson J, Saykally R, Morris N, Pham J, He R, Choi H J, 2002 *Adv. Funct. Mater.* **12** 323
[25] Kong X Y, and Wang Z L, 2004 *Appl. Phys. Lett.* **84** 975
[26] Wang X D, Ding Y, Summers C J, Wang Z L, 2004 *J. Phys. Chem. B,* **108** 8773